ACS APPLIED MATERIALS & INTERFACES

Research Article

www.acsami.org

Plasma-Enhanced Chemical Vapor Deposition of *n*-Heptane and Methyl Methacrylate for Potential Cell Alignment Applications

Annina Steinbach,[†] Andrea Tautzenberger,[‡] Andreas Schaller,[†] Andreas Kalytta-Mewes,[†] Sebastian Tränkle,[†] Anita Ignatius,[‡] and Dirk Volkmer*[,†]

[†]Chair of Solid State Chemistry, Institute of Physics, Universitätstrasse 1, 86159 Augsburg, Germany

[‡]Institute of Orthopaedic Research and Biomechanics, Centre of Musculoskeletal Research Ulm, Helmholtzstrasse 14, 89081 Ulm, Germany

Supporting Information

ABSTRACT: Plasma-enhanced chemical vapor deposited polymers (plasma polymers) are promising candidates for biomaterials applications. In the present study, plasma deposition as a fast and easily scalable method was adapted to deposit coatings from *n*-heptane and methyl methacrylate monomers onto glass substrates. Linear patterns with line and groove widths between 1.25 and 160 μm were introduced by degrative UV-lithography for cell alignment. Differential interference contrast optical microscopy, profilometry and atomic force microscopy revealed that the patterned surfaces had a smooth, homogeneous appearance and a pattern height of 8 and 45 nm for plasma deposited *n*-heptane and methyl methacrylate, respectively. UV-lithography increased the oxygen content on the surface drastically as shown by X-ray photoelectron spectroscopy. After immersion in simulated body fluid for 21 days, the pattern was still intact, and the ester groups were also maintained for the most part as shown by infrared spectroscopy. To test the coatings' potential applicability for biomaterial surfaces in a preliminary experiment, we cultured murine preosteoblastic MC3T3-E1 cells on these coatings. Light and electron microscopically, a normal spindle-shaped and aligned cell morphology was observed. At the mRNA level, cells showed no signs of diminished proliferation or elevated expression of apoptosis markers. In conclusion, plasma-enhanced chemical vapor deposited polymers can be patterned with a fast and feasible method and might be suitable materials to guide cell alignment.

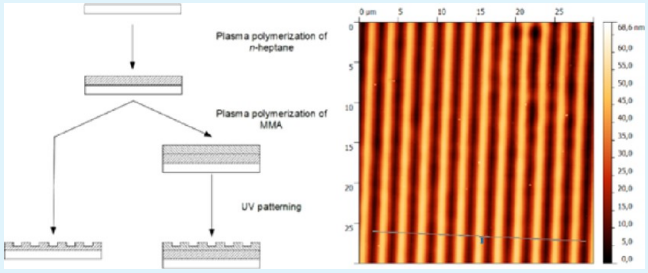

KEYWORDS: *biomaterials, thin films, plasma enhanced chemical vapor deposition (PE-CVD), plasma polymers, micropatterning, MC3T3-E1*

INTRODUCTION

For many years now, polymers deposited using plasma-enhanced chemical vapor deposition (PE-CVD) have been proposed for a whole range of biomaterial applications.[1−3] Drug release, prevention of leaching and corrosion, or a stealth effect for endoprostheses are thought possible as well as usage in the development of lab-on-a-chip devices.[1−3] In the process, a multitude of polymers deposited in a low-temperature plasma have been investigated as model systems.[2−4]

PE-CVD is applicable on many organic monomers, which are not polymerizable using wet chemistry methods. Thus, polymers can be synthesized from simple alkanes such as hexane.[5] Nevertheless, the chemical composition of the monomer is crucial for choosing the polymerization conditions and for the properties of the polymer after the deposition. Aiming at polymers with a specific surface chemistry, such as carboxyl groups or ester groups, monomers containing the corresponding moieties are chosen for polymerization.[6] To avoid fragmentation of the monomer and, therefore, loss of the functional groups during the polymerization process, soft polymerization conditions, i.e., low discharge power and/or pulsed plasma mode, are necessary.[3,5,7−10] When employing soft conditions, it is favorable to use monomers with a double bond in order to achieve adequate deposition rates.[5] However, cross-linking of the monomers is not as high as with high power discharge and using continuous plasma mode.[8,9]

Methyl methacrylate (MMA) has been chosen for this work as a monomer, because MMA is suitable for soft PE-CVD and is estimated to give a poly(methyl methacrylate) (PMMA)-like coating.[10] PMMA is known to be an inert polymer, which has been proven to be biocompatible.[11] It is generally used as bone cement and as a model system for biomaterial research.[12−14] Additionally, spin-coated PMMA films provide a good surface for a protein distribution to encourage cell adhesion.[15]

It is also well-known that cells react not only to a favorable protein surface but to topographical cues and align to linear

Received: June 21, 2012
Accepted: September 19, 2012
Published: September 19, 2012

structures as well.[16−18] Some studies indicated even a beneficial effect of these geometrical patterns on cell adhesion behavior and cell-surface integration.[19,20] These geometrical cues could be provided by substrates produced by PE-CVD.

In the present study, the feasibility of PE-CVD as a method for biomaterials production was tested. It promises simple upscaling, and involves neither complex synthesis nor extensive handling of samples. Therefore, the bone cement monomer MMA was deposited onto model glass surfaces by PE-CVD giving a nanolayer of plasma polymerized methyl methacrylate (ppMMA). Coating stability in an ionic environment was evaluated by immersion in simulated body fluid (SBF). To provide stability in SBF, we inserted plasma-polymerized *n*-heptane (ppH) as an adhesion promoting layer. Additionally, ppH was tested on its own as a single layer system (compare Figure 1). The coatings were micropatterned with lines by UV-

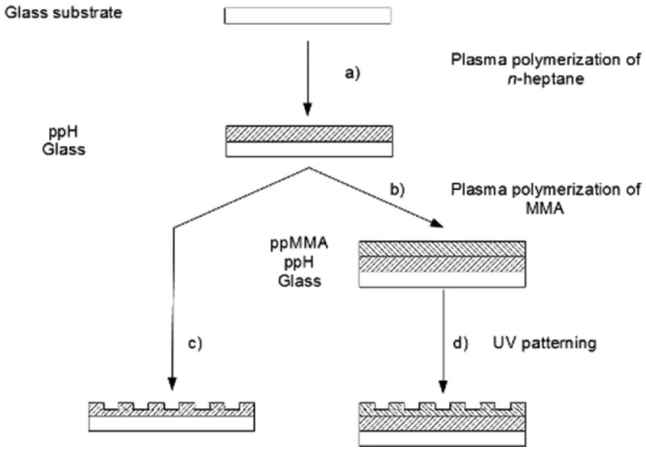

Figure 1. Schematic of the coating process showing the process's steps leading to the polymer layers used for the experiments in this work. Cleansed glass substrates were coated with (a) plasma-polymerized heptane (ppH) by PE-CVD of *n*-heptane and either furnished with (b) a layer of plasma-polymerized MMA (ppMMA) and (d) patterned, or (c) directly patterned by UV-lithography.

lithography. To preliminarily test the coatings' potential relevance for biomaterial surfaces, we grew preosteoblastic MC3T3-E1 cells on these materials and examined their morphology as well as their proliferation and viability.

EXPERIMENTAL SECTION

Preparation of Patterned Plasma Polymer Coatings. The steps of the coating preparation are shown schematically in Figure 1. Etching and polymerization processes were conducted using a FEMTO low-pressure plasma system (Diener electronic, Germany). The chamber volume is approximately 6 dm^3. The maximum power output of the generator was 300 W at a frequency of 40 kHz in pulsed or continuous mode. A homogeneous plasma was obtained, because the gas and monomers were distributed uniformly by several gas inlets. The pressure in the reaction chamber was adjusted via mass flow controllers using gases or by a shutter using liquid monomers. Gases were taken from gas bottles without further purification, liquid monomers were fed into the chamber from an evaporator which was kept at a constant temperature of 30 °C. The pressure given for each plasma process refers to the pressure after ignition of the plasma. Between polymerization processes with different monomers the chamber was cleansed with oxygen plasma.

Before coating, the coverslips (Menzel, Germany) were etched in argon/hydrogen plasma for 30 min at 300 W power output in the continuous mode. During etching, the flow rates of argon and hydrogen (gas mixing ratio 82/18) were adjusted to keep the pressure in the reaction chamber at 0.3 mbar.

Immersion experiments showed that ppMMA layers delaminated from the glass surface when exposed to simulated body fluid (SBF) for 21 days as described below. Therefore, the samples were coated with a layer of ppH acting as an adhesion promoting agent. Polymerization of *n*-heptane (Figure 1 a) was carried out directly after the etching process without removing the glass coverslips from the reaction chamber to avoid contamination of the samples. During polymerization of *n*-heptane for 1 h, power output was 90 W in pulsed mode and the pressure was adjusted to 0.5 mbar. Before the next polymerization step (Figure 1 b), after removing the samples, the chamber was cleansed with oxygen plasma using 300 W power output and a pressure of 0.5 mbar. Deposition of ppMMA was carried out using pulsed mode and a pressure of 0.5 mbar for 30 min at 150 W power output.

The conditions for plasma polymerization described here, such as power output, process duration, and pressure, were adjusted in the optimization process to receive polymer layers that were transparent and stable in SBF for 21 days.

The resulting polymer layers were patterned by UV-lithography (Figure 1c, d), employing a Hamamatsu LC8 (Japan) containing a 250 nm enhanced 200 W mercury lamp. The optical power integrated from 250 to 2200 nm reaching the samples after its way through our optical setup with a synthetic silica light guide and a beam distributor was 328 mW/cm^2. The coatings were irradiated through a quartz mask with the respective linear pattern for 20 min. The custom-made patterned quartz masks' design is described in detail by Letsche.[21] After the irradiation, the substrates were rinsed with deionized water.

In vitro Bioactivity and Stability Test in Simulated Body Fluid. As described by Kokubo et al.,[22] SBF was designed to mimic in vitro the conditions of in vivo biomaterial studies. It is therefore used to try in vitro to predict a material's behavior in vivo, e.g., if it promotes biomineralization even in an acellular environment. In this study, however, immersion in SBF was also used to screen diverse plasma polymer coatings produced with different adhesion promoting layers and by differing procedures for their stability in ion solutions.

The SBF was prepared in a Tris-HCl buffer at pH 7 by solving the salts in the amounts given in Table S2 in the Supporting Information to add up to the corresponding ion concentrations.[22] The SBF was autoclaved, and the samples and vessels were washed with 70% ethanol to prevent bacterial contamination and possibly resulting artifacts. The test was run for 3 weeks at 37 °C in tightly closed Teflon vessels with the samples standing in an upright position.

Analysis of Coatings. Successful and uniform coating and patterning was verified by inspection of the patterned samples with an Olympus IX70 light microscope (Germany) operated in the differential interference contrast (DIC) mode.

To determine the pattern height, a Dektak profilometer (Bruker, Germany) was employed. Scans were performed at three different positions of a substrate. Of each scan, five steps were evaluated. The reported pattern height refers to the mean value.

For a more detailed analysis, the pattern height and surface morphology were observed by atomic force microscopy (AFM). AFM measurements were conducted with an Agilent 5500 Scanning Probe Microscope (USA) under ambient conditions. The data was collected via tapping mode (acoustic AFM) in closed loop configuration with a large multipurpose closed-loop scanner. Olympus cantilevers (OMCL-AC160TS) with a tetrahedral tip (typical spring constant of 42 N/m, typical tip-radius of 7−10 nm) and resonance frequencies ranging from 300 to 340 kHz were used. The plasma polymer coatings were scanned at a speed of 0.5−0.6 lines per second with a resolution of 512 × 512 pixels. Open-source scanning probe microscopy data analysis software 'Gwyddion'[23] was employed for handling the topographical data and extraction of profiles.

Additionally, attenuated total reflectance infrared (ATR-IR) spectra of nonpatterned samples before and after immersion in SBF were collected in order to investigate the stability of the ppMMA layer. Basically, the signal of the ester moiety served as an indicator for the stability of the polymer. ATR-IR measurements were conducted using

an Equinox 55 FT-IR-spectrometer (Bruker, Germany). Unpolymerized MMA was used without further preparation as a reference. Spectral data was evaluated using the program 'OriginPro 8.5.0G' (OriginLab Corporation, USA).

X-ray photoelectron spectroscopy (XPS) measurements were conducted using an Omicron system with an Al Kα X-ray source. For the measurements, the plasma polymer films were deposited on conductive highly oriented pyrolytic graphite (HOPG) substrates. CasaXPS software was employed for analysis of the data fitting the spectra with pseudo-Voigt profiles assuming equal profile width.

Cell Culture and Analysis of Cell Morphology. Cells of the murine preosteoblastic cell line MC3T3-E1 (German Collection of Microorganisms and Cell Cultures, Germany) were cultured in α-minimal essential medium (Biochrom, Germany) with 10% fetal calf serum (PAA Laboratories, Germany), 4 mM L-glutamine, 100 U/mL penicillin and 0.1 mg/mL streptomycin (all from Biochrom, Germany) at 37 °C, 5% CO_2 and saturated humidity as described before.[24] For the experiment, MC3T3-E1 cells were seeded at 1×10^4 per cm^2 onto cell culture plastic and the ppMMA or ppH plasma polymer substrates (line patterns with 10 or 50 μm width) in 12 well cell culture plates and were cultured for 21 days with medium changes twice a week.

Live cells were examined for their morphology with a DMI6000 B light microscope (Leica, Germany). Images were taken with a DFC420C camera (Leica, Germany) at days 1, 3, 7 and 21.

Cell morphology was analyzed more closely by SEM at day 21. Sample preparation was carried out as described previously.[24] Images were taken with a scanning electron microscope (SEM; S-5200, Hitachi Europe GmbH, Germany) at an accelerating voltage of 10 kV.

Real-Time Reverse Transcriptase Polymerase Chain Reaction (Real-Time RT-PCR). Real-time RT-PCR (StepOnePlus™ Real-Time PCR System, Applied Biosystems, Germany) was performed to determine quantitative effects on mRNA expression as described in detail before.[24] Specific primer pairs (Thermo Electron GmbH, Germany) are listed in Table S3 in the Supporting Information. Data analysis (normalized to glyceraldehyde-3-phosphate dehydrogenase (GAPDH) and related to the cell culture plastic control) was performed according to the ΔΔCt (cycle threshold) method,[25] with the corresponding calculation steps specified in Steinbach et al.[24]

The experiment and the measurements were performed in duplicate, respectively, resulting in a number of data values $n = 4$. mRNA expression data are expressed as mean ± standard deviation. Statistical analysis was omitted because of the small amount of data.

RESULTS AND DISCUSSION

Plasma Deposition and Coating Analysis. Two different polymer coatings on glass slides were prepared by PE-CVD of *n*-heptane and MMA: ppMMA as the outer layer and ppH serving as an adhesion promoting agent, or ppH as a single layer system. The preparation of the polymer layers and their patterning is depicted schematically in Figure 1. It was optimized to an all-plasma process, requiring minimum handling and transferring the samples. The process is intended to be applicable for up-scaled processes with larger sample throughput. The resulting coatings were tested for their potential suitability as biomaterials coatings.

For the polymer film synthesis, pulsed plasma mode was chosen to reduce the concentration of free radicals in the ppH layers and to avoid cleavage of the MMA monomers.[8] In compliance with this, in ATR-IR measurements, the ester signal at 1726 cm^{-1} of the monomer MMA (dashed line in Figure 2) was also detected after PE-CVD in the resulting coating (dotted line). This clearly indicated that the functional group was not strongly affected by the plasma conditions applied, and could still be found in the polymer. Both spectra − of MMA and ppMMA − are in accordance with database spectra for MMA and PMMA, respectively, with regard to the main band positions.[26] The general broadening of bands for plasma

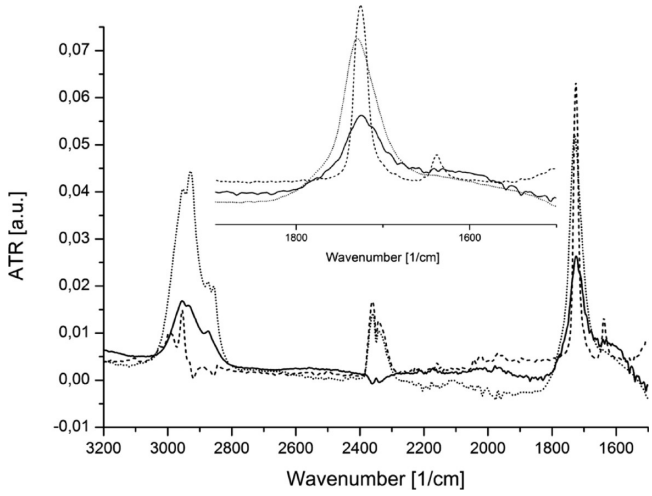

Figure 2. ATR-IR spectra of the monomer MMA (dashed line) and the coating resulting from PE-CVD of MMA (dotted line) with an adhesion promoting layer made of ppH. After immersion in SBF for 21 days, these substrates showed the IR spectrum indicated by the solid line. The inset depicts the signal of the ester group in detail.

polymers[7,10] is also observed here and is based on the less defined chemical surrounding compared to the monomer and conventional polymers.[8] The reaction in the plasma led to an increase of signals between 2800 and 3000 cm^{-1}. This hints at the formation of C−H bonds with neighboring alkene moieties.[7] At the same time, the well-defined signal of the C−C double bond at 1638 cm^{-1} disappeared with polymerization. This is probably due to formation of C−C single bonds through addition polymerization.[5]

XPS analysis revealed a certain loss of the ester moiety, which manifests in a slightly higher ratio of the C−O double bond environment at 536.8 eV to the C−O single bond environment at 538.1 eV in the fitted O 1s high resolution spectrum (Figure 3). Instead of the 1:1 ratio expected for the conventional PMMA, the ratio is 56.9% to 43.1% with an excess of double bonds. This is anticipated for ppMMA due to a plasma induced scission of the ester between the carboxyl C and the methoxyl group.[10] This is reflected by the peak at 291.9 eV assigned to the carbonyl environment in the fitted C 1s high-resolution spectrum additional to the alkyl peak at 289.6 eV, the methoxyl peak at 291.0 eV, and the carboxyl peak at 293.6 eV. The charging of the sample is accounted for the shift of the peaks to higher values compared to literature.[10] Relative peak positions, however, are consistent.

The success of the coating and patterning procedure was also examined light microscopically in the DIC mode (see Figure S1 in the Supporting Information) and by AFM (Figure 4). The coatings were optically very homogeneous across the whole sample and showed no signs of pinholes or other irregularities even in the nanometer sampling range of the AFM (Figure 4). As can be seen in Figure 4, the coatings could be patterned with lines comprising size features as small as 1.25 μm by UV-lithography. The pattern height depended on the upmost polymer. As determined by profilometry, ppMMA coatings had an average pattern height of 45 nm, whereas for coatings consisting only of a ppH layer, the UV-irradiation process resulted in only 8 nm pattern height. This can be seen as an analogue to the "conventional" polymers polyethylene (PE), as a hydrocarbon polymer, and PMMA. PE resists UV-degradation better than other polymers, as it lacks chromo-

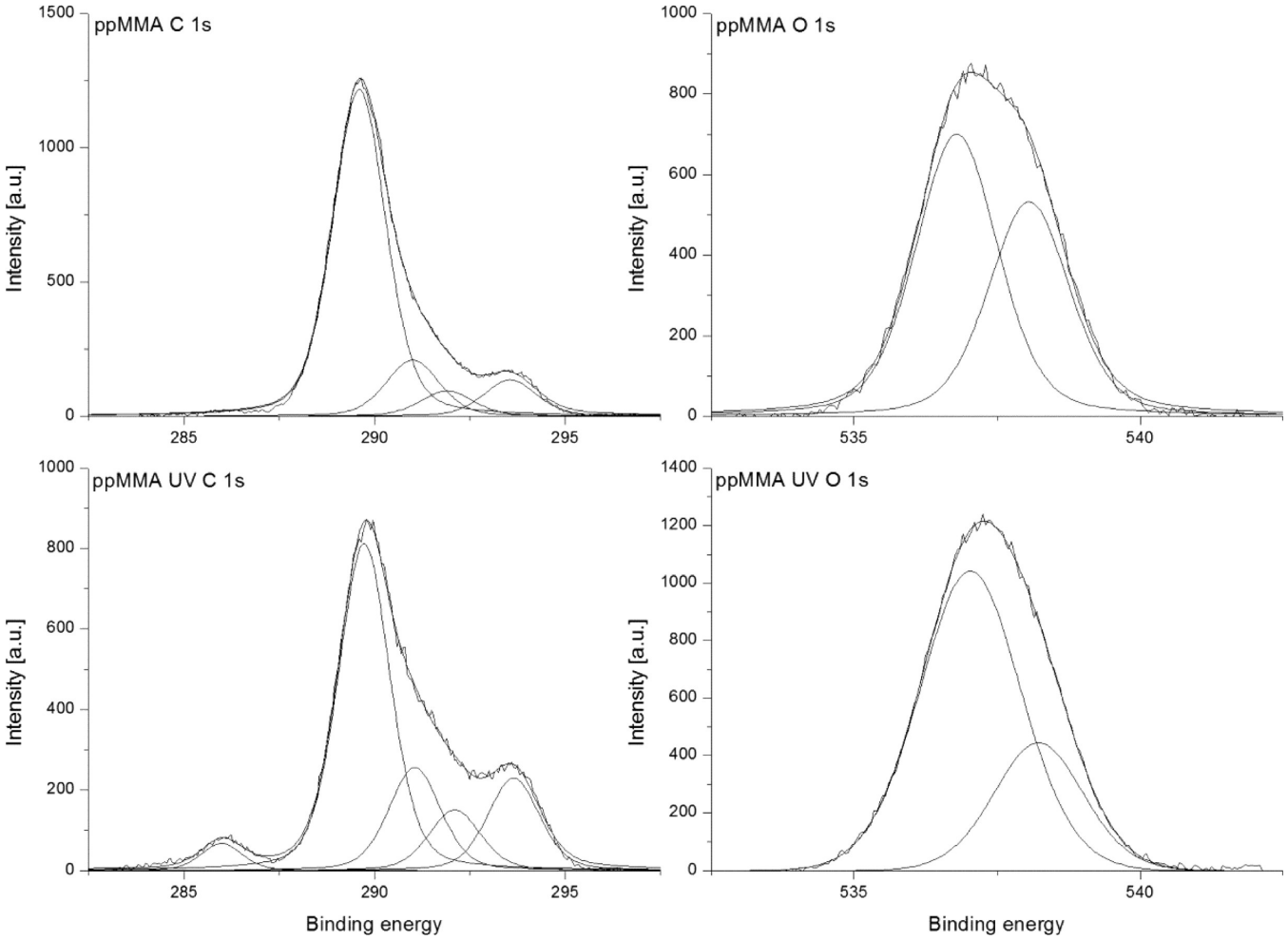

Figure 3. Fitted high-resolution C 1s (left column) and O 1s (right column) XPS spectra for the ppMMA before (upper row) and after UV-ablation (lower row).

phoric groups.[27] Whereas PMMA also resists quite well UV-irradiation due to its short ester side groups, it is nevertheless prone to degradation by a photoinduced ester decomposition process and might be photo-oxidized. Assuming that the plasma polymers act in an analogous manner, the UV-lithography of PMMA should result in the formation of acid groups, possibly followed by cross-linking.[28]

XPS results supported an oxidation process showing the oxygen content to increase from 21.5% before the UV-irradiation to 29.0% after the irradiation. Fitting the high-resolution C 1s spectrum resulted in 44% oxygen binding C species compared to 26.5% before the irradiation. The fitted high resolution O 1s spectrum in Figure 3 shows that the ratio of the double bond drastically increases to 72.6% of the oxygen species. This points at a high rate of an ester decomposition process with a loss of the methoxyl group, probably resulting in carbonyl moieties, which can account for the high double bond excess over the single bond environment.

As the plasma polymer layers should not delaminate in an aqueous environment in view of cell culture application, the coatings were screened for their stability and possible bioactivity in vitro by immersion in SBF for 21 days. Delamination was observed, when styrene was used as the monomer for the adhesion promoting layer, or when no additional layer was introduced (data not shown). These layer constructions were consequently abolished. Delamination was not observed for ppH coatings and ppMMA with a ppH adhesion promoting layer. The stability of plasma-polymerized thin films seems to depend on the density of (hydrophilic) functional groups in the polymer layer and on its solubility in water.[29] Therefore the stability can be improved by an appropriate adhesion promoting layer. Often, adhesion promoting layers are self-assembled monolayers, which form a covalent bond to the surface on the one side and provide a hydrocarbon tail on the other side. The hydrocarbon tail can participate in the plasma reaction and provide a linkage between substrate and coating.[8,17] Plasma-polymerizing another monomer, as it was applied here, is also a suitable route to bridge the chemistries of substrate and coating.[30] Another possibility is the "dilution" of moieties such as carboxylates with simple hydrocarbons.[29,31] Although PMMA is not hydrophilic, the ester moieties seemed to add enough polar properties to delaminate the thin films in an aqueous environment. Why, despite its general hydrophobic properties,[32] plasma-polymerized styrene was not suitable as adhesion promoting layer might deserve further investigations.

The integrity of the coatings after immersion in SBF was verified by AFM scans (Figure 5). The topography did not change discernibly for the macroscopically stable coatings, which was taken as a token for their stability in ion containing media. There were no cracks or holes to discern, which could have indicated disintegration of the polymer layers. The pattern

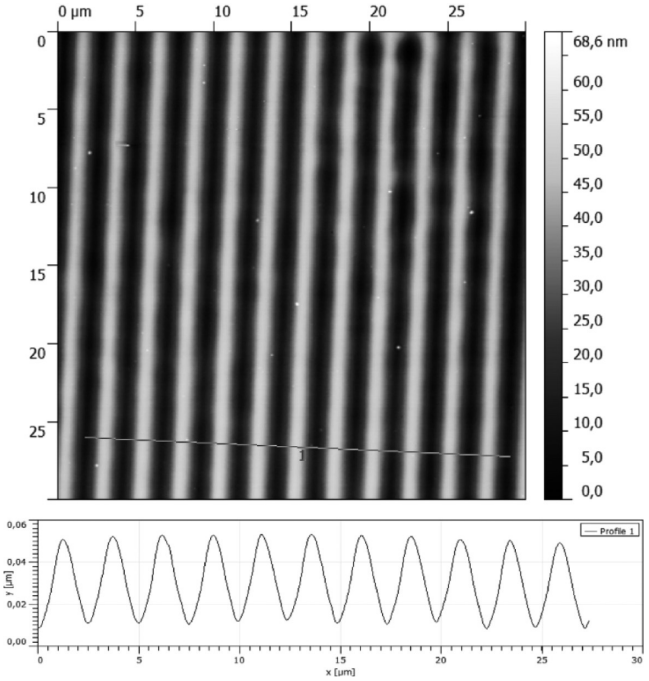

Figure 4. AFM topography of a ppMMA sample UV-irradiated through a photomask with a linear pattern with a line width of 1.25 μm for 20 min, below the profile corresponding to the line indicated in the topographical image.

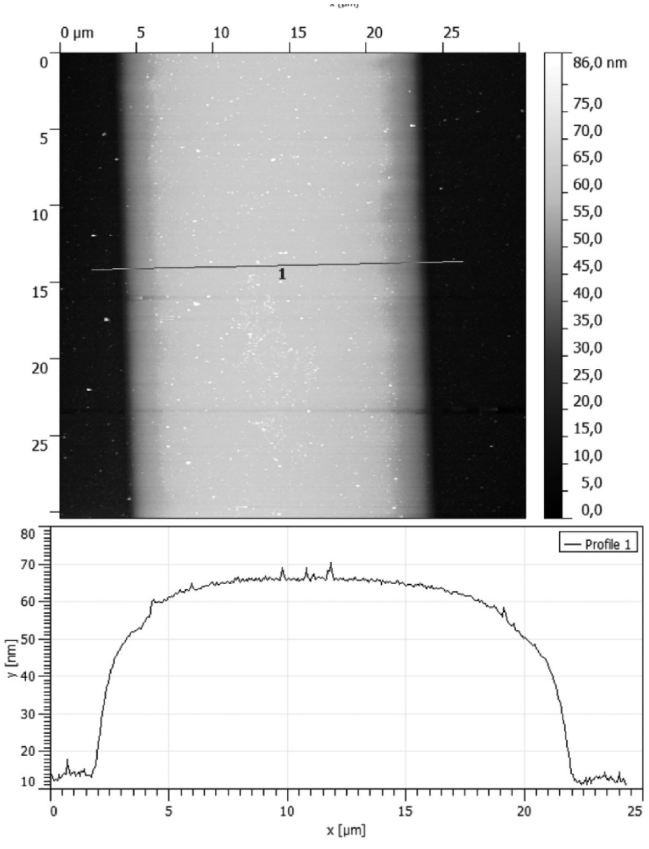

Figure 5. AFM topography of a ppMMA sample after 21 days immersion in SBF with the profile below, the position of which is marked by the line in the topographical image.

height was also maintained after the immersion, as can be seen in the profile in Figure 5. This observation was supported by ATR-IR measurements. Figure 2 shows that the signal associated with esters at 1726 cm^{-1} was still clearly detectable and had the same width as the ppMMA coating prior to immersion (compare solid and dotted line in Figure 2). It might be added that a quantitative conclusion cannot be drawn, because the signal height strongly depended on sample positioning, which determined contact pressure and angle of the ATR crystal.

Despite the stability tests in SBF conducted before, the formation of cracks (Figure 6C, H) and cavities (Figure 6J, O, and T) was discovered during the cell experiments on the sample with larger pattern. However, the pattern on all substrates was still visible at day 21. Accordingly, no delamination took place. This hints at strains in the layer due to swelling in an ion containing aqueous environment. Additional support for this assumption is gleaned from the fact that this was only observed for the larger pattern, as the smaller patterns allow for an easier lateral dilatation in case of swelling.[8]

As described by Kokubo et al.,[22] immersion in SBF is a first in vitro test to indicate possible material behavior in vivo. Materials, which are suitable for applications in bone, promote biomineralization, even without bone building cells being present. Thus, after the immersion, the samples were examined under the microscope for signs of biomineralization. However, none of the coatings showed signs of mineral being formed under these biomineralization conditions, which might have been an indication of possible bioactivity in this context.[22,33]

Biomineralization might be induced by alternative functional groups, such as carboxylates, phosphates, or sulfates.[34,35] The feasibility of further functionalizing[2] the here produced polymers with the low temperature plasma technique opens up numerous possibilities in synthesis. Also other moieties could be introduced, e.g., nitrogen-containing groups to realize additional antibacterial properties.[36]

Cell Colonization and Proliferation. To test the biocompatibility and effects on bone cell morphology or proliferation, preosteoblastic MC3T3-E1 cells were cultured on ppH and ppMMA samples. Based on previous experiments,[24] line widths of 10 and 50 μm were chosen for these cell experiments.

As can be observed in Figure 6, the cells proliferated well and to the same degree on the test surfaces as on the cell culture plastic control in the course of 21 days (reading the panel from the left to the right, comparing the different surfaces in the panel rows). After 7 days of cell culture (Figure 6K–O), MC3T3-E1 cells completely covered the plasma polymer substrates independently of the monomer used to produce the samples.

The unaffected proliferation was confirmed by real-time RT-PCR results (Table 1). Here, the mRNA expression of a marker of apoptosis (tumor protein P53) and two proliferation markers (antigen identified by monoclonal antibody Ki-67 and histone H4) in cells on the patterned substrates was compared to the expression of cells on the control substrate, which was set at 1. At the mRNA level, no harmful influence of the polymer coatings was detected in this preliminary experiment.

Therefore, these data encourage further experiments in the future. Good proliferation leads to a high cell density, which induces the differentiation of osteoblasts.[37] It is also known that cell–cell contacts are beneficial for the viability of MC3T3-E1

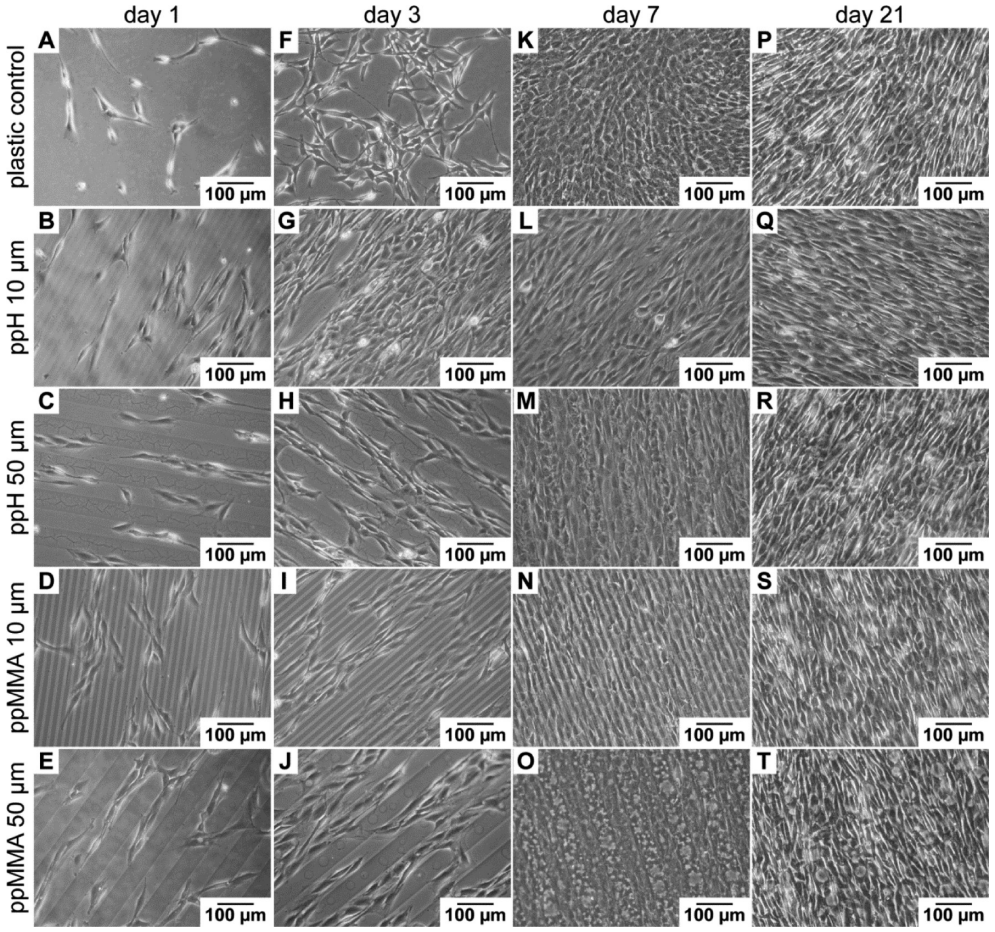

Figure 6. Cell morphology of MC3T3-E1 cells on day 1, day 3, day 7, and day 21 (A–E, F–J, K–O, and P–T, respectively), on the plastic control, the ppH coating with 10 and 50 μm line width, and the ppMMA coating with 10 and 50 μm line width (rows from top to bottom).

Table 1. mRNA Expression of Apoptosis and Proliferation Markers in MC3T3-E1 Cells[a]

	gene of interest		
substrate	*P53*	*Ki-67*	*H4*
ppH line pattern with 10 μm width	0.90 ± 0.02	1.62 ± 0.39	1.06 ± 0.15
ppH line pattern with 50 μm width	0.91 ± 0.06	2.09 ± 0.08	1.20 ± 0.02
ppMMA line pattern with 10 μm width	0.87 ± 0.01	1.04 ± 0.08	0.75 ± 0.07
ppMMA line pattern with 50 μm width	0.75 ± 0.04	1.25 ± 0.17	0.65 ± 0.10

[a]mRNA expression of the apoptosis marker tumor protein P53 (*P53*), of the proliferation markers antigen identified by monoclonal antibody Ki-67 (*Ki-67*), and histone H4 (*H4*), in MC3T3-E1 cells cultured on the ppH and ppMMA substrates with line patterns with 10 μm width and 50 μm widths relative to the mRNA expression on the cell culture plastic control at day 21 of the experiment. Via the ΔΔCt (cycle threshold) method, levels of mRNA were normalized to glyceraldehyde-3-phosphate dehydrogenase mRNA levels and related to the mRNA expression on the cell culture plastic control (mRNA expression on cell culture plastic was set at 1), n = 4.

cells.[38] Therefore, a coating material for biomaterials should promote the good proliferation rate and cell density we in fact observed for these plasma deposited polymers.

Noticeably, unlike the cells on the control substrate (Figure 6, first row of the panel), the MC3T3-E1 cells on the coated glass slides coaligned with the linear pattern from day 1 to day 21 on all patterned substrates (Figure 6, rows 2–5). These cells showed an elongated and well-spread morphology that was confirmed by SEM (see Figure S2 in the Supporting Information) and is a sign for good adhesion. The extracellular matrix clearly visible between the cells on all substrates is yet another sign for a regular cell growth and function.

Although geometrical shapes, such as the linear pattern used here, are simplified model patterns compared to the natural environment of osteoblasts,[39,40] these patterns yet have practical relevance. Eisenbarth et al.[19] revealed that aligned MC3T3-E1 cells on structured surfaces had a better adhesion behavior and formed more focal contacts than cells on polished substrates with a more spherelike appearance. The cells' orientation also seems to determine the orientation of the collagenous matrix they secret[41] and through this also mineralization[42,43] as well as the mechanical properties[44,45] in bone. With these findings in mind, it is not surprising that micro- and nanotopographies are proposed for applications as biomaterials to guide osteoblast adhesion and alignment.[46]

CONCLUSION

The results of the present study implicate, that ppH and ppMMA coatings prepared by PE-CVD are promising materials for future biomaterials applications. The method is straightforward and requires handling the samples only when loading and unloading the plasma chamber. Thus, it should be easily adaptable for scalable processing. This work also showed that

the SBF test as established by Kokubo et al. can be used off the road to screen different coatings for their stability in simulated physiological environments.

In addition, a preliminary cell culture experiment encourages further investigations with a view to biomaterials applications. Murine preosteoblastic MC3T3-E1 cells grew well, aligned to the linear pattern right from day 1 over the complete period of culture, and showed no signs of increased apoptosis or reduced proliferation at mRNA level compared to cells on the cell culture plastic control.

■ ASSOCIATED CONTENT

Supporting Information

Table of chemicals used for PE-CVD including lot numbers, table of the ion concentrations in SBF, table of the primer sequences used for real-time RT-PCR, table of the fitting results of the high-resolution C 1s and O 1s spectra, DIC micrograph of the substrates used for cell culture, and SEM images of the cells' morphology at day 21. This material is available free of charge via the Internet at http://pubs.acs.org/.

■ AUTHOR INFORMATION

Corresponding Author

*E-mail: dirk.volkmer@physik.uni-augsburg.de.

Author Contributions

The manuscript was written through contributions of all authors. All authors have given approval to the final version of the manuscript.

Notes

The authors declare no competing financial interest.

■ ACKNOWLEDGMENTS

The expert technical assistance of Helga Bach and the valuable help of Ray Frenzel are gratefully acknowledged.

■ ABBREVIATIONS

AFM, atomic force microscopy; ATR-IR, attenuated total reflectance infrared; DIC, differential interference contrast; *H4*, *histone H4*; *Ki-67*, antigen identified by monoclonal antibody Ki-67; MMA, methyl methacrylate; *P53*, tumor protein P53; PE, polyethylene; PE-CVD, plasma-enhanced chemical vapor deposition; PMMA, poly(methyl methacrylate); ppH, plasma-polymerized *n*-heptane; ppMMA, plasma-polymerized methyl methacrylate; real-time RT-PCR, real-time reverse transcriptase polymerase chain reaction; SBF, simulated body fluid; UV, ultraviolet light; XPS, X-ray photoelectron spectroscopy

■ REFERENCES

(1) Yasuda, H.; Gazicki, M. *Biomaterials* **1982**, *3*, 68−77.
(2) Desmet, T.; Morent, R.; Geyter, N. D.; Leys, C.; Schacht, E.; Dubruel, P. *Biomacromolecules* **2009**, *10*, 2351−2378.
(3) Pryce Lewis, H. G.; Edell, D. J.; Gleason, K. K. *Chem. Mater.* **2000**, *12*, 3488−3494.
(4) Ball, V.; Del Frari, D.; Michel, M.; Buehler, M. J.; Toniazzo, V.; Singh, M. K.; Gracio, J.; Ruch, D. *BioNanoSci.* **2012**, *2*, 16−34.
(5) Yasuda, H.; HSU, T. *J. Polym. Sci., Polym. Chem. Ed.* **1977**, *15*, 81−97.
(6) Suffner, J.; Schechner, G.; Sieger, H.; Hahn, H. *Chem. Vap. Deposition* **2007**, *13*, 459−464.
(7) Gengenbach, T. R.; Griesser, H. J. *J. Polym. Sci, Part A: Polym. Chem.* **1998**, *36*, 985−1000.
(8) Förch, R.; Zhang, Z.; Knoll, W. *Plasma Processes Polym.* **2005**, *2*, 351−372.
(9) Limb, S. J.; Edell, D. J.; Gleason, E. F.; Gleason, K. K. *J. Appl. Polym. Sci.* **1998**, *67*, 1489−1502.
(10) Casserly, T. B.; Gleason, K. K. *Chem. Vap. Deposition* **2006**, *12*, 59−66.
(11) Santavirta, S.; Konttinen, Y. T.; Bergroth, V.; Grönblad, M. *Acta Orthop. Scand.* **1991**, *62*, 29−32.
(12) DiMaio, F. R. *Orthopedics* **2002**, *25*, 1399−1407.
(13) Oonishi, H.; Akiyama, H.; Takemoto, M.; Kawai, T.; Yamamoto, K.; Yamamuro, T.; Oonishi, H.; Nakamura, T. *Acta Orthop.* **2011**, *82*, 553−558.
(14) Lampin, M.; Warocquier-Clerout, R.; Legris, C.; Degrange, M.; Sigot-Luizard, M. *J. Biomed. Mater. Res.* **1997**, *36*, 99−108.
(15) Alaerts, J.; Cupere, V. D.; Moser, S.; van den Bosh de Aguilar, P.; Rouxhet, P. *Biomaterials* **2001**, *22*, 1635−1642.
(16) Zahor, D.; Radko, A.; Vago, R.; Gheber, L. *Mater. Sci. Eng., C* **2007**, *27*, 117−121.
(17) Ploux, L.; Anselme, K.; Dirani, A.; Ponche, A.; Soppera, O.; Roucoules, V. *Langmuir* **2009**, *25*, 8161−8169.
(18) Charest, J. L.; Eliason, M. T.; García, A. J.; King, W. P. *Biomaterials* **2006**, *27*, 2487−2494.
(19) Eisenbarth, E.; Linez, P.; Biehl, V.; Velten, D.; Breme, J.; Hildebrand, H. F. *Biomol. Eng.* **2002**, *19*, 233−237.
(20) Soboyejo, W. O.; Nemetski, B.; Allameh, S.; Marcantonio, N.; Mercer, C.; Ricci, J. *J. Biomed. Mater. Res.* **2002**, *62*, 56−72.
(21) Letsche, S. A., Dissertation, University of Ulm, 2012.
(22) Kokubo, T.; Kushitani, H.; Sakka, S.; Kitsugi, T.; Yamamuro, T. *J. Biomed. Mater. Res.* **1990**, *24*, 721−734.
(23) Nečas, D.; Klapetek, P. *Cent. Eur. J. Phys.* **2012**, *10*, 181−188.
(24) Steinbach, A.; Tautzenberger, A.; Ignatius, A.; Pluntke, M.; Marti, O.; Volkmer, D. *J. Mater. Sci.: Mater. Med.* **2012**, *23*, 573−579.
(25) Livak, K. J.; Schmittgen, T. D. *Methods* **2001**, *25*, 402−408.
(26) Spectral Database for Organic Compounds SDBS, spectra No. 1425 MMA and 4062 PMMA http://riodb01.ibase.aist.go.jp/sdbs
(27) Gijsman, P.; Meijers, G.; Vitarelli, G. *Polym. Degrad. Stab.* **1999**, *65*, 433−441.
(28) Soeriyadi, A. H.; Trouillet, V.; Bennet, F.; Bruns, M.; Whittaker, M. R.; Boyer, C.; Barker, P. J.; Davis, T. P.; Barner-Kowollik, C. *J. Polym. Sci., Part A: Polym. Chem.* **2012**, *50*, 1801−1811.
(29) Robinson, D. E.; Buttle, D. J.; Whittle, J. D.; Parry, K. L.; Short, R. D.; Steele, D. A. *Plasma Processes Polym.* **2010**, *7*, 102−106.
(30) Timmons, R. B.; Griggs, A. J. Pulsed Plasma Polymerizations. In *Plasma Polymer Films*; Biedermann, H., Ed.; ICP: London, 2004; pp 217−245.
(31) Daw, R.; Candan, S.; Beck, A.; Devlin, A.; Brook, I.; MacNeil, S.; Dawson, R.; Short, R. *Biomaterials* **1998**, *19*, 1717−1725.
(32) Topala, I.; Asandulesa, M.; Spridon, D.; Dumitrascu, N. *IEEE Trans. Plasma Sci.* **2009**, *37*, 946−950.
(33) Thiang, E. S.; Huang, J.; Best, S. M.; Barber, Z. H.; Bonfield, W. *J. Biomed. Mater. Res., Part. B* **2006**, *76*, 326−333.
(34) Arias, J. L.; Neira-Carrillo, A.; Arias, J. I.; Escobar, C.; Bodero, M.; David, M.; Fernández, M. S. *J. Mater. Chem.* **2004**, *14*, 2154−2160.
(35) Liu, Q.; Ding, J.; Mante, F. K.; Wunder, S. L.; Baran, G. R. *Biomaterials* **2002**, *23*, 3103−3111.
(36) Zhang, W.; Wang, H.; Oyane, A.; Tsurushima, H.; Chu, P. K. *Biomed. Mater. Eng.* **2011**, *21*, 75−82.
(37) Kim, Y. S.; Birge, S. J.; Avioli, L. V.; Miller, R. *Calcif. Tissue Int.* **1987**, *41*, 218−222.
(38) Tsutsumimoto, T.; Kawasaki, S.; Ebara, S.; Takaoka, K. *J. Bone Miner. Res.* **1999**, *14*, 1751−1760.
(39) Weiner, S.; Wagner, H. *Annu. Rev. Mater. Sci.* **1998**, *28*, 271−298.
(40) Webster, T. J.; Ahn, E. S. *Adv. Biochem. Eng. Biotechnol.* **2006**, *103*, 275−308.
(41) Wang, J.H.-C.; Jia, F.; Gilbert, T. W.; Woo, S.L-Y. *J. Biomech.* **2003**, *36*, 97−102.
(42) Saito, M.; Soshi, S.; Fuji, K. *J. Bone Min. Res.* **2003**, *18*, 1695−1705.
(43) Meier, C.; Welland, M. E. *Biomacromolecules* **2011**, *12*, 3453−3459.

(44) Buehler, M. J. *Proc. ASME–Int. Mech. Eng. Congr. Expo.* **2009**, 795–798.
(45) Zhu, B.; Lu, Q.; Yin, J.; Hu, J.; Wang, Z. *Tissue Eng.* **2005**, *11*, 825–836.
(46) Kenar, H.; Kocabas, A.; Aydinli, A.; Hasirci, V. *J. Biomed. Mater. Res., Part A* **2008**, *85*, 1001–1010.